

The complete genome sequence of *Pantoea ananatis* AJ13355, an organism with great biotechnological potential

Yoshihiko Hara · Naoki Kadotani · Hiroshi Izui · Joanna I. Katashkina · Tatiana M. Kuvaeva · Irina G. Andreeva · Lyubov I. Golubeva · Dmitry B. Malko · Vsevolod J. Makeev · Sergey V. Mashko · Yurii I. Kozlov

Received: 20 September 2011 / Revised: 23 October 2011 / Accepted: 5 November 2011 / Published online: 10 December 2011
© The Author(s) 2011. This article is published with open access at Springerlink.com

Abstract *Pantoea ananatis* AJ13355 is a newly identified member of the Enterobacteriaceae family with promising biotechnological applications. This bacterium is able to grow at an acidic pH and is resistant to saturating concentrations of L-glutamic acid, making this organism a suitable host for the production of L-glutamate. In the current study, the complete genomic sequence of *P. ananatis* AJ13355 was determined. The genome was found to consist of a single circular chromosome consisting of 4,555,536 bp [DDBJ: AP012032] and a circular plasmid, pEA320, of 321,744 bp [DDBJ: AP012033]. After automated annotation, 4,071 protein-coding sequences were identified in the *P. ananatis* AJ13355 genome. For 4,025 of these genes, functions were assigned based on homologies

to known proteins. A high level of nucleotide sequence identity (99%) was revealed between the genome of *P. ananatis* AJ13355 and the previously published genome of *P. ananatis* LMG 20103. Short colinear regions, which are identical to DNA sequences in the *Escherichia coli* MG1655 chromosome, were found to be widely dispersed along the *P. ananatis* AJ13355 genome. Conjugal gene transfer from *E. coli* to *P. ananatis*, mediated by homologous recombination between short identical sequences, was also experimentally demonstrated. The determination of the genome sequence has paved the way for the directed metabolic engineering of *P. ananatis* to produce biotechnologically relevant compounds.

Keywords Central carbon metabolism · Interspecies conjugation · Genome backbone · Genome sequencing · Genome synteny · Megaplasmid

Yurii I. Kozlov is deceased.

Electronic supplementary material The online version of this article (doi:10.1007/s00253-011-3713-5) contains supplementary material, which is available to authorized users.

Y. Hara · N. Kadotani · H. Izui
Fermentation and Biotechnology Laboratories, Ajinomoto Co., Inc.,
1-1 Suzuki-cho, Kawasaki-ku,
Kawasaki 210-8681, Japan

J. I. Katashkina · T. M. Kuvaeva · I. G. Andreeva ·
L. I. Golubeva (✉) · D. B. Malko · V. J. Makeev · S. V. Mashko ·
Y. I. Kozlov
Ajinomoto-Genetika Research Institute,
1st Dorozhny Pr. 1-1,
Moscow 117545, Russia
e-mail: luba_golubeva@agri.ru

Present Address:
D. B. Malko · V. J. Makeev
Vavilov Institute of General Genetics RAS,
Gubkina str. 3,
Moscow 119991, Russia

Introduction

In the mid-1990s, specialists from the Ajinomoto Co., Inc. (Kawasaki, Japan), collected a gram-negative acidophilic bacterium from the soil of a tea plantation in Iwata-shi (Shizuoka, Japan), which was designated as strain AJ13355. This bacterium has proven to be capable of growing on a variety of sugars and organic acids at acidic and neutral pH values, and it is resistant to high concentrations of L-glutamic acid (L-Glu) (Moriya et al. 1999). According to standard microbiological tests on its bacteriological properties and nucleotide sequencing of its 16S rRNA (Kwon et al. 1997), this strain was identified as *Pantoea ananatis* (Takahashi et al. 2008).

The natural resistance of the AJ13355 strain to saturating L-Glu concentrations was used to pinpoint promising L-Glu

producers using metabolically engineered *P. ananatis* strains and to develop an L-Glu fermentation process at an acidic pH accompanied by product precipitation (Izui et al. 2006). Other studies have indicated the potential for exploiting AJ13355-based engineered strains for overproduction of L-aspartic acid (Mokhova et al. 2010) and the other strains belonging to the *Pantoea* genus to produce cytotoxic and antiproliferative compounds (Kamimura et al. 1997; Page et al. 1999), 2,3-butanediol (Jiang 2007), pyrogallol (Zeida et al. 1998), glycerol (Dodge and Valle 2009), L-DOPA (Kumagai et al. 2008), such vitamins as carotenoids and vitamin E (Yoon et al. 2007; Albermann et al. 2008), pyrroloquinoline quinone (PQQ) (Andreeva et al. 2011), and ascorbic acid intermediates (Dodge and Valle 2009).

These findings encourage a practical interest in basic research on the structure of the *P. ananatis* AJ13355 genome, the metabolic features of this strain, and tools for genetically manipulating the bacterium.

Previously, a set of high-performance methods for the target modification of *P. ananatis* chromosome (such as deletion or insertions of genetic material, nucleotide change, modification of regulatory region, and construction of unmarked mutations) based on the site-specific and homologous recombination of phage λ , together with the possible transfer of marked mutations by electroporation of the chromosomal DNA, were adapted to genetically engineer *P. ananatis* AJ13355 and its derivatives (Katashkina et al. 2009). Recently, the method for in vivo cloning of large fragments of *P. ananatis* chromosome followed by its amplification via “Dual In/Out technology” (Minaeva et al. 2008) was developed (see, for more details, Andreeva et al. 2011). In the current study, the *P. ananatis* AJ13355 genome was sequenced and annotated.

Materials and Methods

Bacterial strains and plasmids

The strains and plasmids used in the present study are shown in Table 1.

Recombinant DNA techniques

All DNA manipulations were performed according to standard procedures (Sambrook and Russell 2001). λ Red-driven modifications of the *P. ananatis* AJ13355 chromosome were completed according to previously developed methods (Katashkina et al. 2009).

Genome sequencing and annotation

Bacterial cultures of *P. ananatis* AJ13355 were grown in Luria–Bertani (LB) medium and were subsequently used to

isolate genomic DNA using the Qiagen Genomic-Kit (Qiagen K.K., Tokyo, Japan).

Small-insert and large-insert *P. ananatis* AJ13355 DNA libraries were constructed after cloning fragments of 1–3 or 30–40 kb in length, which were obtained by partial digestion with *Sau*3A and purified by gel electrophoresis using low-melting agarose into the pUC18 plasmid or SuperCos 1 cosmid vector (Stratagene, La Jolla, CA), respectively. Sequencing was performed using either a DYEnamic ET Terminator Cycle Sequencing Kit (Amersham Pharmacia Biotech UK, Buckinghamshire, UK) or a BigDye Terminators with an ABI Prism 3700 DNA Analyzer (Applied Biosystems Japan, Tokyo, Japan). Obtained sequences were assembled into contigs using Clustering and Alignment Tool (CAT) software (Hitachi, Ltd., Tokyo, Japan).

Based on the end-sequence data from the obtained libraries, direct linkages between the contigs were estimated using CAT software, and linking cosmid clones were selected from the large-insert library. To fill the gaps between the contigs, sequences of the inserted fragments of the selected clones were determined using the primer-walking method. To determine the nucleotide sequences of the remaining gaps between the contigs, *P. ananatis* genomic DNA was amplified by polymerase chain reaction (PCR) using primers designed from the end sequences of the contigs, and the amplified products were directly sequenced by primer walking.

The edited *P. ananatis* AJ13355 genome sequences were uploaded in FASTA format and annotated.

Protein-coding sequences (CDSs) were predicted using GLIMMER software (Kasif et al. 1999), with an initial construction of the training model by sequence alignment of the genomes of *P. ananatis* and the reference strain *Escherichia coli* MG1655 using MAUVE software (Darling et al. 2010). The gene positions and their functional annotations were transferred from the reference to the *P. ananatis* AJ13355 genome based on strongly homologous regions to create the training model. Identified CDSs were compared against a nonredundant protein sequence database using TBLASTN (<http://ncbi.nlm.nih.gov>) software or using SwissProt database (<http://www.uniprot.org>) in cases of a low level of homology or *P. ananatis*-specific regions. Only the hits with an *e* value of less than 10^{-10} and a protein-length coverage of more than 75% were used. For each homologous region, the best hits were considered to be the sources of the functional annotations. Noncoding RNA predictions were performed using a framework for noncoding RNA detection (Raasch et al. 2010). Finally, all predictions were combined to produce a genome annotation and were checked by visual inspection to correct for gene starts and to reject false-positive predicted genes.

Table 1 Bacterial strains and plasmids

	Relevant characteristics	Reference
Strains		
<i>P. ananatis</i> AJ13355	Wild type	FERM BP-6614 ^a
<i>P. ananatis</i> SC17	Derivative of AJ13355, which produces a low amount of exopolysaccharide	Izui et al. 2003
<i>P. ananatis</i> IZ130	<i>sucA</i> ::Km; Km ^R	Moriya et al. 1999
<i>E. coli</i> K12 MG1655	Wild type	VKPM ^b
<i>E. coli</i> K12 MG1655 <i>abrB</i> :: <i>oriT</i>	<i>abrB</i> :: <i>oriT</i> (Cm ^R)	This study
<i>E. coli</i> S17-1	<i>pir</i> ⁺ strain (Tp ^R Sm ^R <i>recA</i> , <i>thi</i> , <i>pro</i> , <i>hsdR</i> ⁺ M ⁺ , RP4: 2-Tc:Mu:Km Tn7 <i>λpir</i>) used as a recipient strain for maintenance of <i>pir</i> -dependent plasmids	de Lorenzo and Timmis 1994
Plasmids		
pUT399	Origin of replication of γ R6K, RP4 <i>oriT</i> , <i>mobA</i> , <i>mobB</i> , Δ <i>mobC</i> , Cm ^R	Zhang and Meyer 1997
pUT399- <i>abrB</i>	pUT399 derivative carrying <i>E. coli</i> <i>abrB</i> region	[DDBJ: AB610285]
pRK2013	<i>oriColE1</i> RK2- <i>mob</i> ⁺ RK2- <i>tra</i> ⁺ ; Km ^R ; a helper plasmid for the mobilization of non-self-transmissible plasmids	Figurski and Helinski 1979
pMW118-(<i>λattL-tetA-tetR-λattR</i>)	pMW118 (GenBank accession number AB005475)-based plasmid; Ap ^R , Tc ^R	Minaeva et al. 2008

^aInternational Patent Organism Depository

^bRussian National Collection of Industrial Microorganisms at the Institute of Genetics and Selection of Industrial Microorganisms (WDCM No. 588)

Comparative genome analysis

MAUVE software, a dot-matcher tool from the EMBOSS package (Rice et al. 2000), BLAST software (<http://ncbi.nlm.nih.gov>), and homemade Perl scripts were used for genome comparison and finding orthologous CDSs. The plasmids were linked to the end of the linearized chromosome of a corresponding *Pantoea* strain for easy understanding of the differences in the genomic structures.

For CDSs, found orthologues were linked to their genome position to evaluate synteny (i.e., a conserved order of orthologous CDSs between the compared genomes). For the generation of a Venn diagram, CDSs possessing an amino acid identity higher than 30% were defined as orthologues.

Construction of the *E. coli* Hfr strain

An *oriT* site was introduced into the *E. coli* MG1655 chromosome in the *abrB* gene, which is located approximately 10 kb upstream of the *sucA* gene. To achieve this insertion, a DNA fragment from the *E. coli* *abrB* gene, flanked by the *EcoRI* and *SmaI* restriction sites, was amplified by PCR using the *E. coli* MG1655 chromosome as a template and using the primers

P1: 5'-gatccccgggatacaccacaaagagaaaataatgagggagc-3' and

P2: 5'-gatcgaattccgcttcggcgcataggtgaaataaacgc-3',

the *SmaI* and *EcoRI* sites are underlined. The amplified DNA fragment was inserted between the *EcoRI* and *SmaI*

sites in the mobilizable, conditionally replicated (*pir*⁺-dependent) plasmid pUT399 (Cm^R), with an origin of replication of γ R6K and *Mob*⁺ locus from RP4 (Zhang and Meyer 1997) to generate pUT399-*abrB* [DDBJ: AB610285]. The *E. coli* MG1655 strain was subsequently transformed by pUT399-*abrB*, and an integrant, MG1655*abrB*::*oriT*, was obtained due to homologous recombination.

Conjugative crossing between *E. coli* and *P. ananatis*

The *E. coli* donor strain (MG1655*abrB*::*oriT*/pRK2013) carrying the conjugative pRK2013 (Km^R) plasmid was cultivated at 37 °C on an LB agar plate. The Tc^R-plasmid carrier *P. ananatis* strain (IZ130/pMW118-(*λattL-tetA-tetR-λattR*)), used as a recipient, was cultivated at 34 °C on an LB agar plate supplemented with 0.5% glucose and 1× M9 salt. Cells of both strains were collected from one fourth of a plate, washed twice with 1 ml of double-distilled water and resuspended in 300 μ l of double-distilled water. Next, a 25- μ l suspension of each strain was mixed and plated on an LB agar plate. After 3 h of incubation at room temperature, the cells were collected, plated on selective medium (M9 containing L-Glu [2 g/L] as the sole carbon source and 12.5 mg/l tetracycline [Tc]) and cultivated at 34 °C. After 1 week of cultivation, L-Glu-assimilating Tc^R-clones were randomly selected, and their chromosome structures were preliminarily checked by PCR using the primers P3: 5'-tgggacgaagagtacccgaacaaag-3' and

P4: 5'-cgctgacaagctggagcaggaaaaa-3'.

Results

Assembly and annotation of the *P. ananatis* AJ13355 genome sequence

The genome of *P. ananatis* AJ13355 was sequenced using the shotgun method. One small-insert plasmid library (1–3 kb) and one cosmid library (30–40 kb) were constructed through the digestion and cloning of the genomic DNA.

Approximately 76,000 samples from the plasmid-based library (corresponding to more than 8.9-fold coverage of the genome size) were sequenced and were assembled using CAT software, which yielded 215 contigs with 96.3% coverage. End sequences from 600 samples of the cosmid-based library (corresponding to a coverage of more than fivefold of the genome size) were assembled using CAT software, which yielded nine contigs with 97.7% coverage. All the sequence and physical gaps were then closed by editing the ends of the sequence traces, primer walking on plasmid clones, and combinatorial PCR, which was followed by sequencing of the PCR product. As a result, two circular DNA molecules were obtained: a 4,555,536-bp chromosome [DDBJ: AP012032] and a 321,744-bp molecule, corresponding to the pEA320 plasmid [DDBJ: AP012033]. Previously, the autonomous replication of pEA320 in *P. ananatis* AJ13355 had been observed experimentally (Hara et al. 2007). General features of the *P. ananatis* genome are summarized in Table 2.

The GC-skew analysis of the *P. ananatis* AJ13355 chromosome, which is generally applicable to the identification of the leading and lagging strands in DNA replication (Grigoriev 1998), indicated bidirectional replication that starts at the proposed *oriC* sequence, near the *mioC* and *gidA* genes (with coordinates 3,803,243–3,803,475 in the sequenced chromosome), and ends close to the calculated replication terminus, around 1.5 Mb (Fig. 1). The 22 genes of the ribosomal RNAs identified in the *P. ananatis* chromosome were grouped into seven *rrn*

operons. These operons are located in the two oppositely replicating halves (replichores) of the chromosome and are transcribed in the direction of replication, as previously demonstrated for several bacterial chromosomes (Blattner et al. 1997; Kunst et al. 1997; Veith et al. 2004).

GLIMMER and TBLASTN software were used to annotate 3,789 CDSs for the *P. ananatis* AJ13355 chromosome. Among these, 3,753 CDSs were homologous to previously annotated proteins.

According to the sequence data, the overall G + C content of the *P. ananatis* AJ13355 chromosome is 53.8% (Table 1), whereas the pEA320 megaplasmid exhibits a G + C content of 53.4%. These values are similar, suggesting that acquisition of the plasmid by *P. ananatis* AJ13355 was not a recent event, unless it was acquired by horizontal transfer from an organism with a similar G + C content.

According to predictions based on GLIMMER and TBLASTN software analysis, the pEA320 plasmid contains 282 CDSs. Among these CDSs, 39% are recognized as hypothetical proteins. GC-skew calculations predicted the location of the pEA320 origin of replication to be around 107 kb. This region contains the *repA* gene, coding for a homologue (64.7%) of the RepFIB replication initiation protein, which is specific for incompatibility group FI plasmids. Putative *parAB* genes were identified upstream of the *repA* gene. It is known that ParAB proteins are involved in the mechanisms of stable inheritance of large, low-copy-number plasmids (Velmurugan et al. 2003).

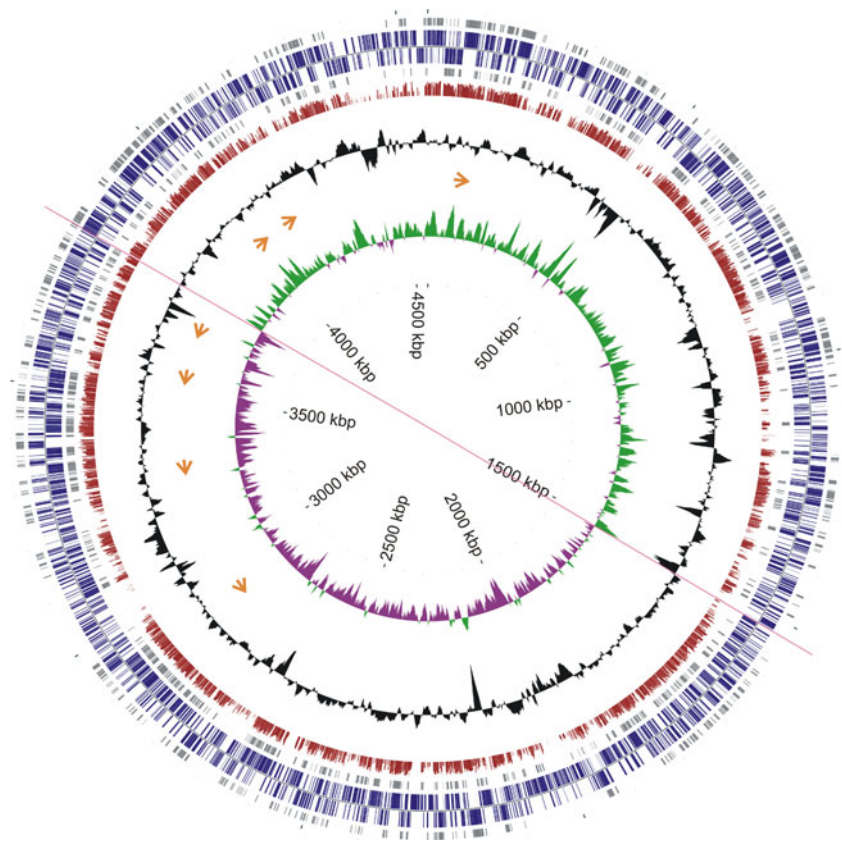
Comparison of the *P. ananatis* AJ13355 genome sequence with that of other members of the *Pantoea* genera

Over the last 3 years, the genomes of three *Pantoea* strains have been sequenced and annotated: *P. ananatis* LMG20103 (De Maayer et al. 2010), *P. vagans* C9-1 (Smits et al. 2010a), and *Pantoea* sp. At-9b (chromosome—NC_014837.1; plasmids—from NC_014838.1 to NC_014842.1). Figure 2 indicates the segments of pronounced colinear similarity between the compared genome pairs at the nucleotide level and suggests that patches of external DNA have been added to a conserved genomic core. Indeed, the genome of *P. ananatis* LMG20103, consisting of a single circular chromosome (4,703,373 bp in length), and the bacterial chromosome of *P. ananatis* AJ13355 share a common “backbone” sequence that is highly colinear, except for one extended region (about 350 kb) that is absent from the chromosome of the latter strain. However, this region of the *P. ananatis* LMG20103 chromosome is highly homologous to the entire autonomously replicated pEA320 plasmid from strain AJ13355 (Fig. 2b). Several homologous regions (about 10 kb long) were also found between pEA320 and chromosome

Table 2 General features of the *P. ananatis* AJ13355 genome

Trait	Chromosome	pEA320
Total size	4,555,536 bp	321,744 bp
G + C content	53.8%	53.4%
CDSs	3,789	282
CDSs encoding annotated proteins	3,753	272
CDSs encoding hypothetical proteins	523	110
Coding density	84.60%	84.64%
Ribosomal RNAs	22	0
Transfer RNAs	78	0

Fig. 1 Circular representation of the *P. ananatis* AJ13355 chromosome. Circles are numbered from 1 (outermost) to 8 (innermost). Circles 2 and 3 show the locations of predicted CDSs on the + and – strands, respectively. Circles 1, 4, and 5 show synteny with the *E. coli* MG1655 chromosome, as follows: circle 1, locations of orthologous CDSs on the + strand; circle 4, locations of orthologous CDSs on the – strand; and circle 5, locations of all *P. ananatis* CDSs orthologous to *E. coli* proteins. Circle 6 shows a G + C content greater and less than the average (0.538) outside and inside the corresponding circle, respectively. Circle 7 shows the positions and direction of transcription of seven *P. ananatis* *rrn* operons. Circle 8 depicts the GC skew (G–C/G + C)



Pantoea sp. At-9b and a chromosome of *P. vagans* C9-1 (data not shown).

P. vagans C9-1 and *Pantoea* sp. At-9b comprise three and five megaplasmids, respectively, in addition to their chromosomal DNA (Table 3). Plasmid pPAG3 from *P. vagans* C9-1 carries at least seven extended fragments (more than 10 kb in length) homologous to pEA320 (Fig. 2d). These homologous regions contain genes and operons that were verified as being expressed from the pPAG3 plasmid and that provide phenotypic features to *P. vagans* C9-1 (Smits et al. 2010b). These features include thiamine and carotenoid biosynthesis and the phosphoenolpyruvate transport system for cellobiose, arbutin, and salicin. The same regions of pPAG3 were found by BLAST-mediated computer search to be homologous to the *P. ananatis* LMG20103 chromosome (data not shown).

An automatic comparison of *P. ananatis* AJ13355 and LMG20103 and *P. vagans* C9-1 was performed at the CDS level, the results of which are summarized in Fig. 3. All three organisms have a core genome of 3140 orthologous CDSs in common. There are 224 CDSs unique to *P. ananatis* AJ13355, 278 CDSs unique to LMG20103, and 1197 CDSs unique to *P. vagans* C9-1. *P. ananatis* AJ13355 shares 634 CDSs with LMG20103 and only 69 CDSs with *P. vagans* C9-1.

Homology between the chromosomes of *P. ananatis* AJ13355 and *E. coli* MG1655

The *P. ananatis* AJ13355 genome was compared with that of *E. coli*, the most examined member of the Enterobacteriaceae family. The total identity of the *P. ananatis* AJ13355 and *E. coli* MG1655 chromosomes at the nucleotide level, as evaluated by BLASTN software, did not exceed 35%. At the same time, this comparative analysis indicated segments of pronounced similarity, which harbor regions of full nucleotide identity for lengths of up to 50 bp. These regions were mainly colinear, except for two extended inversions. Meanwhile, at the nucleotide level, the pEA320 plasmid did not possess any significant homology with the *E. coli* MG1655 chromosome.

A comparative study was undertaken to determine the putative orthologous CDSs between the *P. ananatis* AJ13355 and *E. coli* MG1655 strains. The 702 and 1,723 orthologous CDSs with $\geq 80\%$ and 60%–80% amino acid identity, respectively, between proteins were found based on BLAST and MAUVE software-mediated analysis. There were also 1,146 *P. ananatis* CDSs exhibiting a lower level of homology to *E. coli* proteins (30%–60%). In addition, 219 CDSs from the *P. ananatis* AJ13355 chromosome were

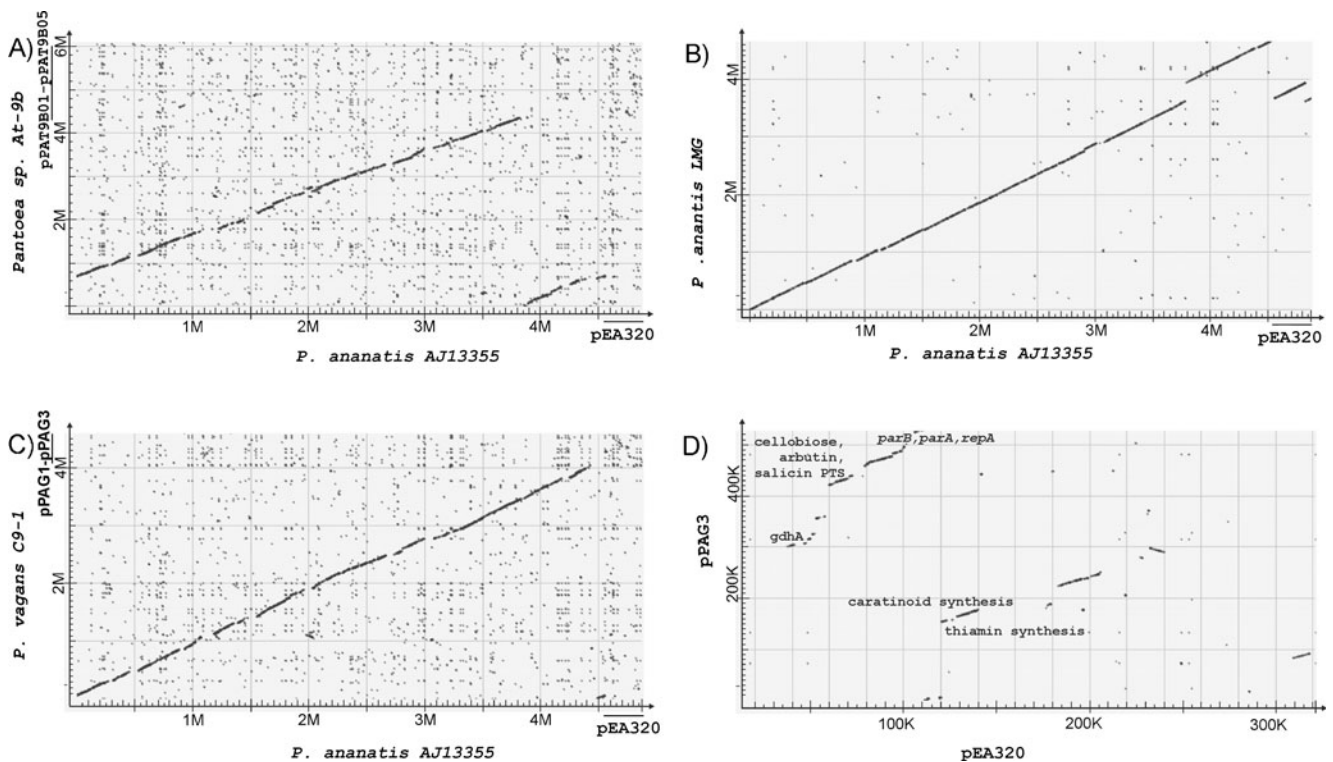


Fig. 2 Two-dimensional similarity plots comparing the nucleotide sequences of the *Pantoea* genomes. The comparison was conducted via BLASTN software using a discontinuous megablast algorithm with default parameters. The plots are as follows: *P. ananatis* AJ13355

versus *Pantoea* sp. At-9b **a**, *P. ananatis* AJ13355 versus *P. ananatis* LMG 20103 **b**, *P. ananatis* AJ13355 versus *P. vagans* C9-1 **c**, and plasmid pEA320 from *P. ananatis* AJ13355 versus plasmid pPAG from *P. vagans* C9-1 **d**

not linked to any homologues in the *E. coli* chromosome (amino acid identity less than 30%).

Although the presence of functional genes tends to be more conserved than the genes positions in different genomes (Huynen and Bork 1998; Lathe et al. 2000), the detected gene content homology also represents synteny between the compared chromosomes of the *P. ananatis* AJ13355 and *E. coli* MG1655 (Fig. 4) strains. In the *P. ananatis* AJ13355 chromosome, 2,285 of 2,425 CDSs, with a level of homology of more than 60% relative to *E. coli* proteins,

are syntenic when placed alongside the MG1655 chromosome. The residual 140 orthologous CDSs are located in two regions of the *P. ananatis* chromosome that appear as inversions when compared with the *E. coli* genome.

The general synteny in gene content homology and the dispersed regions of full nucleotide identity along the genomes of *E. coli* and *P. ananatis* suggested a possible homologous recombination-mediated transfer of large blocks of genes in conjugative interspecific matings, as addressed below.

Table 3 Comparison of the *Pantoea* strains by genome size

<i>Pantoea</i> strain	Size of chromosome (bp)	Megaplasmids (bp)	Total genome size (bp)
<i>P. ananatis</i> AJ13355	4,555,536	pEA320 (321,744)	4,877,280
<i>P. ananatis</i> LMG20103	4,703,373	None	4,703,373
<i>P. vagans</i> C9-1	4,024,986	pPAG1 (167,983) pPAG2 (165,692) pPAG3 (529,676)	4,888,319
<i>Pantoea</i> sp. At-9b	4,368,708	pPAT9B01 (793,935) pPAT9B02 (394,054) pPAT9B03 (321,080) pPAT9B04 (318,111) pPAT9B05 (116,877)	6,312,783

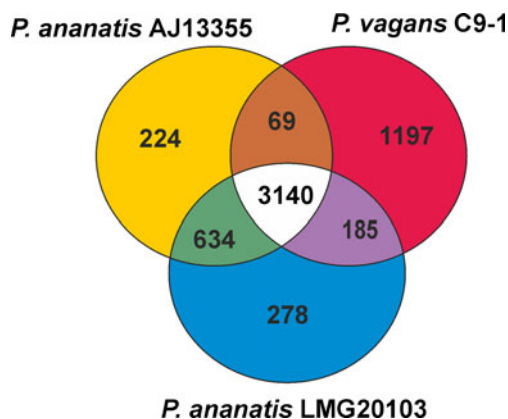


Fig. 3 Protein content comparison of the *P. ananatis* AJ13355, *P. ananatis* LMG 20103, and *P. vagans* C9-1 strains. The Venn diagram shows the number of CDSs shared between two or all three strains by a corresponding intersection of the circles, which represent each organism. CDSs showing more than 30% identity were considered to be orthologues

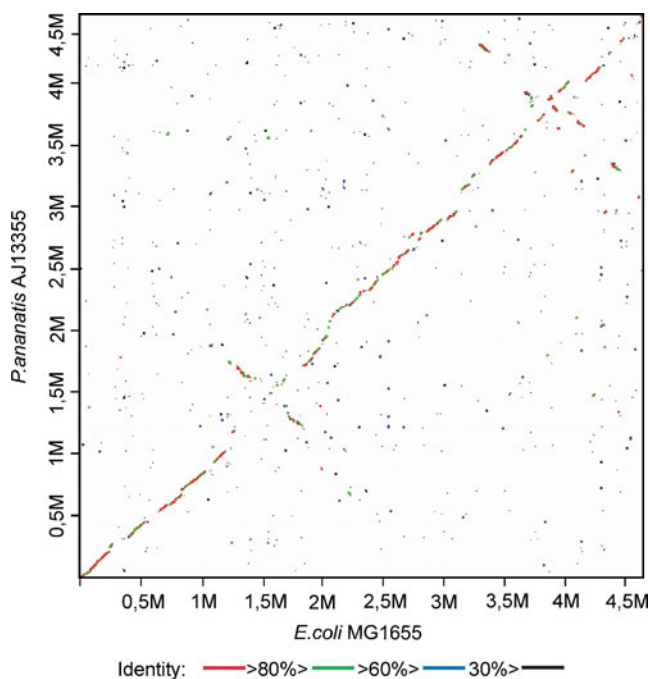


Fig. 4 Synteny between the chromosomes of *P. ananatis* AJ13355 and *E. coli* MG1655. The graph represents an X–Y plot of dots forming syntenic regions between the bacterial chromosomes. Each dot represents a *P. ananatis* CDS with an orthologue in the *E. coli* genome, with coordinates corresponding to the position of the respective region in each chromosome. Orthologous CDSs were detected by reciprocal best BLASTP matches. The color code indicates the amino acid identity in the orthologous CDSs as follows: red, $\geq 80\%$; green, 60%–80%; blue, 30%–60%; and black, $< 30\%$ (nonhomologous proteins)

Conjugative gene transfer between *E. coli* and *P. ananatis*

The *P. ananatis* IZ130 strain could not utilize L-Glu as its sole carbon source due to $\Delta sucA$ -mediated disruption of the tricarboxylic acid cycle. The conjugative-plasmid carrier strain *E. coli* MG1655 *abrB::oriT/pRK2013* was able to transfer the *sucA* gene of the wild type linked with *oriT*. The latter strain, as a donor, and a Tc^R-carrier plasmid strain IZ130/pMW118-($\lambda attL-tetA-tetR-\lambda attR$), as a recipient, were used in a biparental mating experiment. The presence of the Tc^R plasmid in the recipient *P. ananatis* strain provided selection against the donor *E. coli* strain on media containing Tc.

SucA genes in the *P. ananatis* AJ13355 and *E. coli* MG1655 chromosomes are located among syntenic *sdh-suc* CDSs that manifest an additional high level of homology at the level of the nucleotide sequences (Fig. 5a).

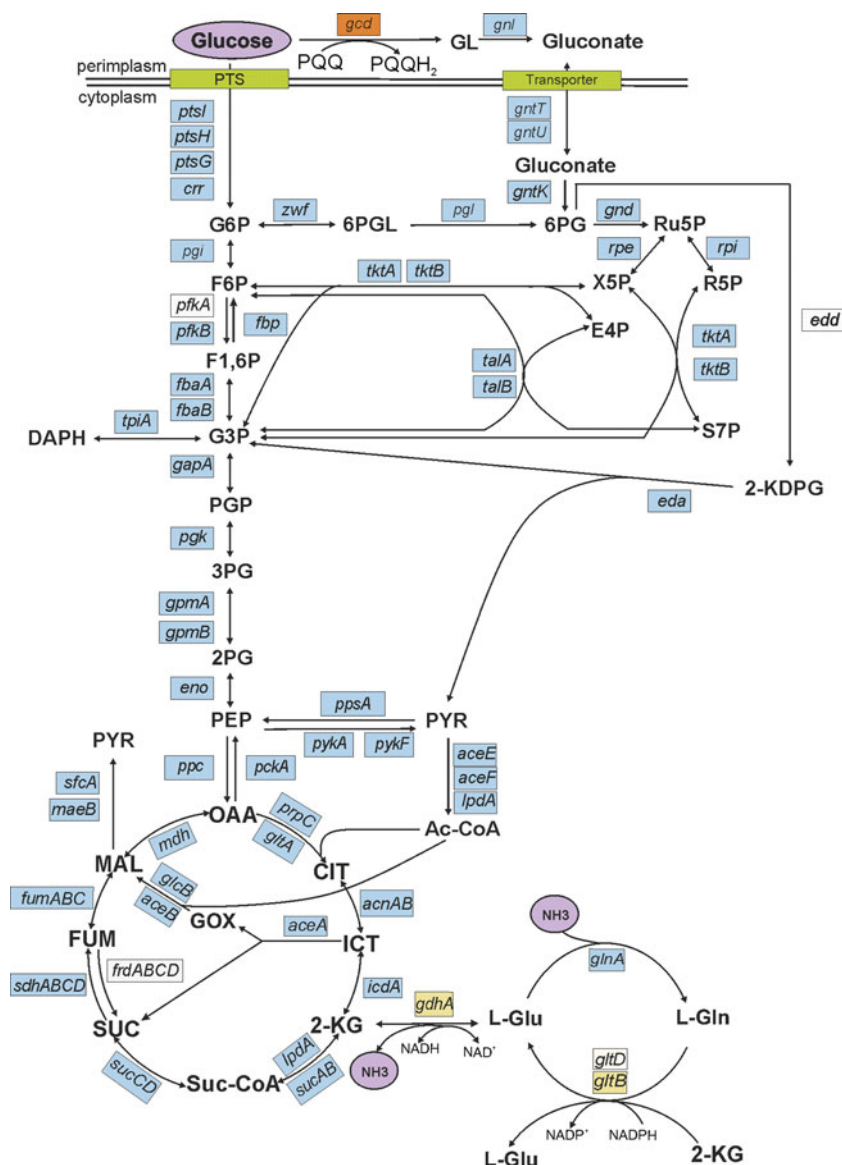
Biparental mating followed by selection of the Tc^R-bacteria on minimal medium with L-Glu as the sole carbon source resulted in recombinant SucA⁺ *P. ananatis* clones at a frequency of approximately 10^{-7} – 10^{-8} . The homologous recombination-mediated replacement of the mutant *P. ananatis* loci by the DNA fragment from the mobilizable *E. coli* chromosome was initially established by PCR analysis and was confirmed by direct DNA sequencing of the 10-kb chromosome region surrounding *sucA* from one of the recombinant clones. According to the data presented in Fig. 5b, the recombination event that resulted in the tested strain had occurred with junctions in the *sdhD* and *sucD* genes of *E. coli* and *P. ananatis*. A nucleotide sequence identity of 11 bp was found between the recombineered chromosomes at the junction points.

Discussion

The determination and annotation of the complete genome sequence of *P. ananatis* AJ13355 have broadened the opportunities for basic research on and goal-directed metabolic engineering of this biotechnologically relevant organism. The present study has established a foundation for proteome and transcriptome analysis, genome-scale reconstruction of metabolic networks based on genome annotation, and valid flux analysis. Together with previously described and applied genetic engineering techniques, the establishment of this organism's annotated genome sequence makes *P. ananatis* AJ13355 an attractive platform organism for the industrial production of organic acids, such as L-Glu and other biotechnologically relevant compounds.

A comparison between *P. ananatis* AJ13355 and earlier sequenced *Pantoea* genomes revealed high structural homology of their nucleotide sequences (Fig. 2) and a large number of shared proteins (Fig. 3). The main

Fig. 6 Proposed similarities and differences in the maps of *E. coli* MG1655 and *P. ananatis* AJ13355 central carbon and ammonia metabolism based on the presence and absence of orthologous CDSs. The following color code was used: blue boxes, homologous CDSs; yellow boxes, CDSs in the *P. ananatis* genome that are not homologous in *E. coli*; orange box, CDS product that is active, due to the existence of the cofactor biosynthetic pathway in the *P. ananatis* genome, but not in *E. coli* K12; and white boxes, *E. coli* genes not found in the *P. ananatis* AJ13355 genome. Used abbreviations for metabolites are included as supplementary material (Table S1). The reaction directions are indicated accordingly to previously published *E. coli* genome-scale metabolic reconstruction (Feist et al. 2007)



be restored after the introduction of the *E. coli edd-eda* operon (Hara et al. 2003).

(3) In *E. coli*, NADPH-dependent glutamate synthase (GOGAT) and ATP-dependent glutamine synthetase (the products of *gltBD* and *glnA*, respectively) and NADPH-dependent glutamate dehydrogenase (GluDH) (encoded by the *gdhA* gene) form two alternative pathways for ammonia assimilation through the amination of α -ketoglutarate to L-Glu (Reitzer 1996). The *P. ananatis* AJ13355 genome does not contain CDSs coding for close homologues of the *E. coli* GOGAT or GluDH. Instead, it contains a putative *gltB* gene (CDS 001_1015 located in the chromosome) encoding a close homologue of the large subunit of GOGAT from *Agrobacterium tumefaciens* and a putative *gdhA* gene (CDS 001_0033 located in the megaplasmid pEA320)

encoding a close homologue of putative NADH-dependent GluDH from *Salmonella typhimurium*. Until now, the dependence of *P. ananatis* GluDH on NADH as a cofactor has been experimentally confirmed (Mokhova et al., in preparation). NADPH-dependent GOGAT and GluDH are among the main consumers of NADPH in *E. coli* cells growing in medium containing ammonia as a nitrogen source (Pramanik and Keasling 1997; Reitzer 1996). The corresponding reactions function mainly to deliver the amino group of the provided L-Glu and glutamine (L-Gln) via transamination to cell mass synthesis and, to a lesser extent, to provide L-Glu and L-Gln for protein synthesis (Reitzer 1996). If the existent NADH-dependent GluDH significantly contributes to ammonia assimilation by *P. ananatis* cells under certain conditions, the carbon flux

distribution among the pathways could significantly differ from the flux distribution in the closely related *E. coli* metabolic network with functional NADPH-dependent GluDH. The latter proposal is based on experimental results obtained for *Corynebacteria* strains that differed in the expression of GluDH with NADH or NADPH cofactor specificities (Marx et al. 1999).

Thus, despite a similar set of metabolic genes present in *P. ananatis* and *E. coli*, several CDSs are unique in these genomes. After being transferred to a heterologous host, the latter CDSs could be useful in improving the performance of metabolically engineered strains based on these closely related, but notably different, bacteria. In addition, these interspecies gene exchanges, probably, could be realized due to the experimentally confirmed conjugative transfer, which is considered as “self-cloning” that is important for the industrial applications of the engineered strains expressing heterologous genes.

Acknowledgments This work was funded by Ajinomoto Co. The authors acknowledge Prof. Andrey A. Mironov for supplying the computer software used in the initial step of the work. They thank Prof. Rustem S. Shakulov for fruitful discussions. A special thanks also goes to Drs. Kiyoshi Matsuno and Shintaro Iwatani for their invaluable suggestions and managerial help during the manuscript preparation.

Open Access This article is distributed under the terms of the Creative Commons Attribution Noncommercial License which permits any noncommercial use, distribution, and reproduction in any medium, provided the original author(s) and source are credited.

References

- Albermann C, Ghanegaonkar S, Lemuth K, Vallon T, Reuss M, Armbruster W, Sprenger GA (2008) Biosynthesis of the vitamin E compound delta-tocotrienol in recombinant *Escherichia coli* cells. *Chembiochem* 9:2524–2533
- Andreeva IG, Golubeva LI, Kuvaeva TM, Gak ER, Katashkina JI, Mashko SV (2011) Identification of *Pantoea ananatis* gene encoding membrane pyrroloquinoline quinone (PQQ)-dependent glucose dehydrogenase and *pqqABCDEF* operon essential for PQQ biosynthesis. *FEMS Microbiol Lett* 318:55–60
- Blattner FR, Plunkett G 3rd, Bloch CA, Perna NT, Burland V, Riley M, Collado-Vides J, Glasner JD, Rode CK, Mayhew GF, Gregor J, Davis NW, Kirkpatrick HA, Goeden MA, Rose DJ, Mau B, Shao Y (1997) The complete genome sequence of *Escherichia coli* K-12. *Science* 277:1453–1462
- Cleton-Jansen AM, Goosen N, Fayet O, van de Putte (1990) Cloning, mapping, and sequencing of the gene encoding *Escherichia coli* quinoprotein glucose dehydrogenase. *J Bacteriol* 172:6308–6315
- Darling AE, Mau B, Perna NT (2010) Progressive Mauve: multiple genome alignment with gene gain, loss, and rearrangement. *PLoS One* 5:e11147
- de Lorenzo V, Timmis KN (1994) Analysis and construction of stable phenotypes in gram-negative bacteria with Tn5- and Tn10-derived minitransposons. *Methods Enzymol* 235:386–405
- De Maayer P, Chan WY, Venter SN, Toth IK, Birch PR, Joubert F, Coutinho TA (2010) Genome sequence of *Pantoea ananatis* LMG20103, the causative agent of *Eucalyptus* blight and dieback. *J Bacteriol* 192:2936–2937
- Dodge T, Valle F (2009) Uncoupled productive and catabolic host cell pathways. European patent 2055773(B1)
- Feist AM, Henry CS, Reed JL, Krummenacker M, Joyce AR, Karp PD, Broadbelt LJ, Hatzimanikatis V, Palsson BO (2007) A genome-scale metabolic reconstruction for *Escherichia coli* K-12 MG1655 that accounts for 1260 ORFs and thermodynamic information. *Mol Syst Biol* 3:121
- Figurski DH, Helinski DR (1979) Replication of an origin-containing derivative of plasmid RK2 dependent on a plasmid function provided in trans. *Proc Natl Acad Sci USA* 76:1648–1652
- Grigoriev A (1998) Analyzing genomes with cumulative skew diagrams. *Nucleic Acids Res* 26:2286–2290
- Hara Y, Izui Hiroshi, Asano T, Watanabe Y, Nakamatsu T (2003) Method for producing L-amino acid. European patent 1352966 (A2)
- Hara Y, Izui H, Noguchi H (2007) Novel plasmid autonomously replicable in Enterobacteriaceae family. European patent 1853621
- Huynen MA, Bork P (1998) Measuring genome evolution. *Proc Natl Acad Sci USA* 95:5849–5856
- Izui H, Hara Y, Sato M, Akiyoshi N (2003) Method for producing L-glutamic acid. US patent 6596517
- Izui H, Moriya M, Hirano S, Hara Y, Ito H, Matsui K (2006) Method for producing L-glutamic acid by fermentation accompanied by precipitation. US patent 7015010
- Jiang XW (2007) Using *Pantoea agglomerans* KFS-9 fungus to produce 2,3-butanediol, and application in cosmetic. Patent application CN1958785(A)
- Kamimura D, Kuramoto M, Yamada K, Yazawa K, Kano M (1997) Oligomycin SC compounds of *Pantoea agglomerans* as anticancer agents. Patent application JP9208587(A)
- Kasif S, White O, Salzberg SL (1999) Improved microbial gene identification with GLIMMER. *Nucleic Acids Res* 27:4636–4641
- Katashkina JI, Hara Y, Golubeva LI, Andreeva IG, Kuvaeva TM, Mashko SV (2009) Use of the λ Red-recombineering method for genetic engineering of *Pantoea ananatis*. *BMC Mol Biol* 10:34. doi:10.1186/1471-2199-10-34
- Kumagai H, Suzuki H, Katayama T, Nawata M, Nakazawa H (2008) Mutant tyrosine repressor, a gene encoding the same, and a method for producing L-DOPA. US patent 7365161
- Kunst F, Ogasawara N, Moszer I, Albertini AM, Alloni G, Azevedo V, Bertero MG, Bessières P, Bolotin A, Borchert S, Borriss R, Boursier L, Brans A, Braun M, Brignell SC, Bron S, Brouillet S, Bruschi CV, Caldwell B, Capuano V, Carter NM, Choi S-K, Codani J-J, Connerton IF, Cummings NJ, Daniel RA, Denizot F, Devine KM, Düsterhöft A, Ehrlich SD, Emmerson PT, Entian KD, Errington J, Fabret C, Ferrari E, Foulger D, Fritz C, Fujita M, Fujita Y, Fuma S, Galizzi A, Galleron N, Ghim S-Y, Glaser P, Goffeau A, Golightly EJ, Grandi G, Guiseppe G, Guy BG, Haga K, Haiech J, Harwood CR, Hénaut A, Hilbert H, Holsappel S, Hosono S, Hullo M-F, Itaya M, Jones L, Joris B, Karamata D, Kasahara Y, Klaerr-Blanchard M, Klein C, Kobayashi Y, Koetter P, Koningstein G, Krogh S, Kumano M, Kurita K, Lapidus A, Lardinois S, Lauber J, Lazarevic V, Lee S-M, Levine A, Liu H, Masuda S, Mauël C, Médigue C, Medina N, Mellado RP, Mizuno M, Moestl D, Nakai S, Noback M, Noone D, O’Reilly M, Ogawa K, Ogiwara K, Oudega B, Park S-H, Parro V, Pohl TM, Portetelle D, Porwollik S, Prescott AM, Presecan E, Pujic P, Purnelle B, Rapoport G, Rey M, Reynolds S, Rieger M, Rivolta C, Rocha E, Roche B, Rose M, Sadaie Y, Sato T, Scanlan E, Schleich S, Schroeter R, Scoffone F, Sekiguchi J, Sekowska A, Seror SJ, Serron P, Shin B-S, Soldo B, Sorokin A, Tacconi E, Takagi T,

- Takahashi H, Takemaru K, Takeuchi M, Tamakoshi A, Tanaka T, Terpstra P, Tognoni A, Tosato V, Uchiyama S, Vandenbol M, Vannier F, Vassarotti A, Viari A, Wambutt R, Wedler E, Wedler H, Weitzenegger T, Winters P, Wipat A, Yamamoto H, Yamane K, Yasumoto K, Yata K, Yoshida K, Yoshikawa H-F, Zumstein E, Yoshikawa H, Danchin (1997) The complete genome sequence of the gram-positive bacterium *Bacillus subtilis*. *Nature* 390:249–256
- Kwon SW, Go SJ, Kang HW, Ryu JC, Jo JK (1997) Phylogenetic analysis of *Erwinia* species based on 16S rRNA gene sequences. *Int J Syst Bacteriol* 47:1061–1067
- Lathe WC 3rd, Snel B, Bork P (2000) Gene context conservation of a higher order than operons. *Trends Biochem Sci* 25:474–479
- Marx A, Eikmanns BJ, Sahn H, de Graaf AA, Eggeling L (1999) Response of the central metabolism in *Corynebacterium glutamicum* to the use of an NADH-dependent glutamate dehydrogenase. *Metab Eng* 1:35–48
- Matsushita K, Arents JC, Bader R, Yamada M, Adachi O, Postma PW (1997) *Escherichia coli* is unable to produce pyrroloquinoline quinone (PQQ). *Microbiology* 143:3149–3156
- Meulenberg JJ, Sellink E, Riegman NH, Postma PW (1992) Nucleotide sequence and structure of the *Klebsiella pneumoniae* *pqq* operon. *Mol Gen Genet* 232:284–294
- Minaeva NI, Gak ER, Zimenkov DV, Skorokhodova AY, Biryukova IV, Mashko SV (2008) Dual-in/out strategy for genes integration into bacterial chromosome: a novel approach to step-by-step construction of plasmid-less marker-less recombinant *E. coli* strains with predesigned genome structure. *BMC Biotechnol* 8:63 doi:10.1186/1472-6750-8-63
- Mokhova ON, Kuvaeva TM, Golubeva LI, Kolokolova AV, Katashkina JY (2010) A bacterium belonging to the genus *Pantoea* producing an L-aspartic acid or L-aspartic acid-derived metabolites. Patent application WO2010038905(A1)
- Moriya M, Izui H, Ono E, Matsui K, Ito H, Hara Y (1999) L-glutamic acid-producing bacterium and method for producing L-glutamic acid. US patent 6331419
- Page M, Landry N, Boissinot M, Helie M-C, Harvey M, Gagne M (1999) Bacterial mass production of taxanes and paclitaxel. Patent application WO9932651(A1)
- Pramanik J, Keasling JD (1997) Stoichiometric model of *Escherichia coli* metabolism: incorporation of growth-rate dependent biomass composition and mechanistic energy requirements. *Biotechnol Bioeng* 56:398–421
- Raasch P, Schmitz U, Patenge N, Vera J, Kreikemeyer B, Wolkenhauer O (2010) Non-coding RNA detection methods combined to improve usability, reproducibility and precision. *BMC Bioinformatics* 11:491
- Reitzer LJ (1996) Ammonia assimilation and biosynthesis of glutamine, glutamate, aspartate, asparagines, L-alanine, and D-alanine. In: Neidhardt FC (ed) *Escherichia coli* and *Salmonella*: cellular and molecular biology, 2nd edn. ASM, Washington, pp 391–407
- Rice P, Longden I, Bleasby A (2000) EMBOSS: the European molecular biology open software suite. *Trends in Genetics* 16:276–277
- Sambrook J, Russell DW (2001) *Molecular cloning: a laboratory manual*, 3rd edn. Cold Spring Harbor laboratory, Cold Spring Harbor
- Smits TH, Rezzonico F, Kamber T, Goesmann A, Ishimaru CA, Stockwell VO, Frey JE, Duffy B (2010a) Genome sequence of the biocontrol agent *Pantoea vagans* strain C9-1. *J Bacteriol* 192:6486–6487
- Smits TH, Rezzonico F, Pelludat C, Goesmann A, Frey JE, Duffy B (2010b) Genomic and phenotypic characterization of a non-pigmented variant of *Pantoea vagans* biocontrol strain C9-1 lacking the 530-kb megaplasmid pPag3. *FEMS Microbiol Lett* 308:48–54
- Takahashi Y, Tateyama Y, Sato M (2008) Process for producing L-glutamic acid US patent 7354744(B2)
- Veith B, Herzberg C, Steckel S, Feesche J, Maurer KH, Ehrenreich P, Bäumer S, Henne A, Liesegang H, Merkl R, Ehrenreich A, Gottschalk GL (2004) The complete genome sequence of *Bacillus licheniformis* DSM13, an organism with great industrial potential. *J Mol Microbiol Biotechnol* 7:204–211
- Velmurugan S, Mehta S, Uzri D, Jayaram M (2003) Stable propagation of ‘selfish’ genetic elements. *J Biosci* 28:623–636
- Yoon SH, Kim JE, Lee SH, Park HM, Choi MS, Kim JY, Lee SH, Shin YC, Keasling JD, Kim SW (2007) Engineering the lycopene synthetic pathway in *E. coli* by comparison of the carotenoid genes of *Pantoea agglomerans* and *Pantoea ananatis*. *Appl Microbiol Biotechnol* 74:131–139
- Zeida M, Wieser M, Yoshida T, Sugio T, Nagasawa T (1998) Purification and characterization of gallic acid decarboxylase from *Pantoea agglomerans* T71. *Appl Environ Microbiol* 64:4743–4747
- Zhang S, Meyer R (1997) The relaxosome protein MobC promotes conjugal plasmid mobilization by extending DNA strand separation to the nick site at the origin of transfer. *Mol Microbiol* 25:509–516